Protein Science (1996), 5:1502–1511. Cambridge University Press. Printed in the USA.

A novel complex of a phenolic derivative with insulin: Structural features related to the T → R transition

G. DAVID SMITH,[1,2] EWA CISZAK,[1] AND WALTER PANGBORN[1]

[1] Hauptman-Woodward Medical Research Institute, Inc., Buffalo, New York 14203
[2] Roswell Park Cancer Institute, Buffalo, New York 14263

(RECEIVED February 21, 1996; ACCEPTED May 2, 1996)

Abstract

The structure of a symmetric $T_3R_3^f$ insulin hexamer, complexed with 4-hydroxybenzamide, has been determined using X-ray crystallographic techniques. Data were measured from six crystals grown in microgravity to a resolution of 1.4 Å and the structure has been refined including the contributions from hydrogen atoms. The crystals are isomorphous with $T_3R_3^f$ complexes of phenolic derivatives as well as with uncomplexed forms. Unlike the structures of complexes with phenol, *m*-cresol, resorcinol, 4′-hydroxyacetanilide, and methylparaben, which bind one phenolic derivative molecule per R- or R^f-state monomer, two molecules of 4-hydroxybenzamide are bound by each R^f-state monomer. The presence of the second guest molecule results in an extensive hydrogen bonding network, mediated by water molecules, between the T- and R^f-state trimers and adds stability to the formation of the hexamer. The only access to these second sites is through three symmetry-related, narrow channels that originate on the surface of the T-state trimer. Although the conformation of the backbone atoms of the monomers is nearly identical to that of other $T_3R_3^f$ hexamers, significant changes are observed in the conformations of side chains in the vicinity of the second binding site. The side chain of the T-state A11 Cys residue, which forms a disulfide bond to A6 Cys in the same monomer, is observed in two discrete conformations; two discrete conformations are also present for the entire A8 Thr residue in the R^f-state monomer. A procedure is also described for an alternate method of interframe scaling and merging intensity data from an image plate detector.

Keywords: 4-hydroxybenzamide; insulin allosterism; $T_3R_3^f$ hexamer; T → R transition; X-ray crystal structure

In recent years, the insulin molecule, which consists of a 21-residue A-chain and a 30-residue B-chain linked by two disulfide bridges, has been shown to be an allosteric protein by both spectroscopic (Kaarsholm et al., 1989; Krüger et al., 1990; Choi et al., 1993; Brzović et al., 1994; Bloom et al., 1995) and crystallographic techniques (Smith et al., 1984; Baker et al., 1988; Derewenda et al., 1989; Smith & Dodson, 1992; Ciszak & Smith, 1994; Smith & Ciszak, 1994; Whittingham et al., 1995). The presence of certain ions or molecules, such as chloride, thiocyanate, or phenolic derivatives, produces a conformational change from extended to α-helical in the first eight residues of the B-chain. In order to distinguish these different conformations, the T and R nomenclature has been used to describe an extended or α-helical conformation, respectively, of the B-chain (Kaarsholm et al., 1989). Thus, the insulin hexamer previously referred to as "2-zinc insulin" (Baker et al., 1988) is designated as T_6, whereas the conformation observed in the presence of phenol is R_6 (Derewenda et al., 1989; Smith & Dodson, 1992). A third conformation has also been observed for which residues B4–B19 are α-helical, with B1–B3 extended, and this conformation has been designated R^f (Ciszak et al. 1995), resulting in a $T_3R_3^f$ hexamer. In the T conformation, a central α-helical region, B9–B19, connects the extended N- and C-terminal segments, whereas the A-chain conformation consists of N- and C-terminal α-helices connected by a short segment with an extended conformation. Although the major conformational change resulting from the T → R transition produces a displacement of the B1 Phe residue by more than 30 Å, smaller displacements are also observed in other portions of the B-chain as well as a rotation of the N-terminal α-helix of the A-chain.

In the presence of chloride or thiocyanate ion, the T → R conformational transition is induced in only three monomers, resulting in a threefold symmetric $T_3R_3^f$ hexamer (Smith et al., 1984; Ciszak & Smith, 1994; Whittingham et al., 1995). Because of the conformational change of the B-chain, an elliptical cavity is generated between two TR^f dimers in the hexamer and is occupied by water molecules; prior to the T → R transition, this site was occupied by a T-state B6 Leu side chain. Spectroscopic and crystallographic studies have shown that inorganic anions alone are incapable of driving the T → R transition to comple-

Reprint requests to: G. David Smith, Hauptman-Woodward Medical Research Institute, Inc., 73 High Street, Buffalo, New York 14203, USA; e-mail: smith@hwi.buffalo.edu.

tion to produce an R_6 hexamer. However, in the presence of an excess of phenol, an R_6 hexamer is produced and crystallographic studies have shown that each of the six elliptical cavities is occupied by a single phenol molecule (Derewenda et al., 1989; Smith & Dodson, 1992). Additional spectroscopic and crystallographic studies have shown that *m*-cresol or resorcinol are also capable of driving the T → R transition to completion (Krüger et al., 1990; Ciszak & Smith, 1992; Choi et al., 1993; Bloom et al., 1995).

However, not all phenolic derivatives bind to all six monomers to form an R_6 hexamer. Larger phenolic derivatives such as methylparaben (Whittingham et al., 1995) and 4′-hydroxyacetanilide (Smith & Ciszak, 1994) generate a $T_3R^f_3$ symmetric hexamer with one phenolic derivative bound by each R^f-state monomer. Although it is possible that the low solubility of these compounds is the limiting factor, spectroscopic studies suggest a negative cooperative effect to be responsible. The binding of phenolic derivatives to three monomers in a trimer is positively cooperative, but the two positively cooperative trimers have been shown to be related by negative cooperativity (Krüger et al., 1990; Brzović et al., 1994; Bloom et al., 1995). The results from crystallographic studies of complexes of insulin with phenol have shown that the phenolic binding site can accommodate considerably larger molecules and it has been noted that a hydrogen bonded network of water molecules extends along a channel that originates near the center of the hexamer toward the guest molecule. However, to date, only water molecules have been found to occupy this secondary site. Spectroscopic studies have also identified 4-hydroxybenzamide and 2,7-dihydroxynaphthalene as additional guest molecules that can bind in the phenolic site and induce the T → R transition to produce an R_6 hexamer (Choi et al., 1993; Bloom et al., 1995).

Reported here is the crystal structure of a $T_3R^f_3$ insulin hexamer that binds six molecules of 4-hydroxybenzamide, two molecules by each R^f-state monomer. This structure provides the first example of an insulin hexamer that binds a phenolic derivative in the secondary phenolic binding site. One cysteine residue (A11) that participates in the intrachain disulfide link in the T-state monomer is observed to be disordered, as is a residue in the A6–A11 loop in the R^f-state monomer, providing further evidence that this loop possesses considerable flexibility. Due to an extensive hydrogen bonding network involving both 4-hydroxybenzamide molecules, additional stability is afforded to the entire $T_3R^f_3$ hexamer and provides an accurate model for further studies involving other phenolic derivatives. The identification of reagents that are more efficient at inducing the T → R transition could ultimately result in insulin preparations with greater stability and slower dissociation rates to the biologically relevant monomer, providing benefits to the diabetic.

Results

Hexamer and dimer stabilization

The asymmetric unit consists of a TR^f insulin dimer and is shown in Figure 1. The three identical dimers that make up the hexamer are related by the crystallographic threefold axis. The two independent zinc ions lie on the crystallographic threefold axis, where they are coordinated by a threefold symmetric T- or R^f-state trimer through the B10 His side chains (Zn-$N^{\epsilon 2}$ unrestrained bond distances of 2.09 and 2.04 Å for the T- and R^f-state monomers, respectively) and add considerable stability to the organization of the hexamer. The octahedral coordination sphere of the T-state zinc ion is completed by three water molecules (Zn-O, 2.27 Å); the R^f-state zinc ion is tetrahedral, and, because the electron density of the fourth coordination site was more than twice that of the B10 His side chain and half that of the zinc, it was assigned as a chloride ion (Zn-Cl, 2.13 Å). The final electron density maps provided no indication of mixed coordination of the T-state zinc ion, as was observed for the uncomplexed $T_3R^f_3$ hexamer (Ciszak & Smith, 1994).

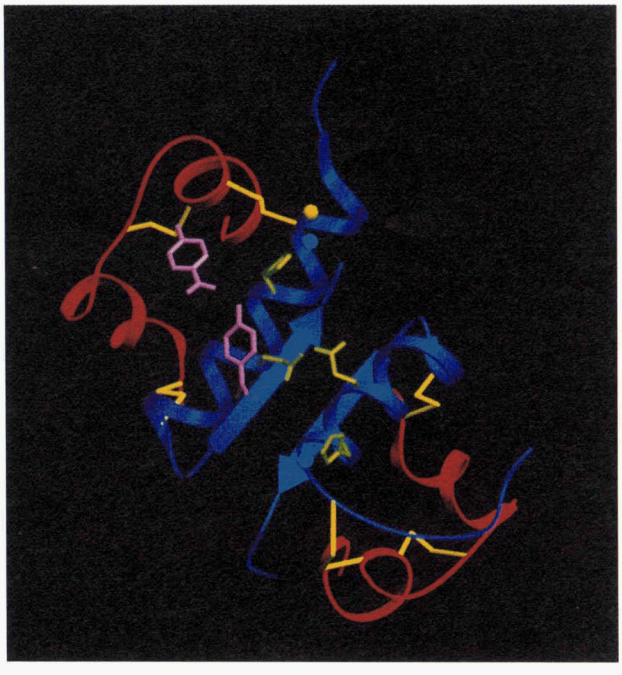

Fig. 1. The TR^f human insulin dimer, represented as a ribbon drawing (Evans, 1993). The R^f-state monomer is on the left side of the drawing. A-chains are colored red; B-chains and zinc ions are blue; the chloride ion, disulfide bonds, B10 His, and B13 Glu side chains are yellow; and the two 4-hydroxybenzamide molecules are pink.

Residues B24–B26 of each monomer in the dimer form a short antiparallel β-pleated sheet and four hydrogen bonds between these strands contribute to dimer stability and are comparable to other native TR^f human insulin dimers. Another hydrogen bonded interaction that contributes to dimer stability is the donation of a proton by the hydroxy group of B9.2 Ser[3] to the carboxyl of B13.1 Glu (O^{γ}-$O^{\epsilon 1}$, 2.92 Å). As a result of the T → R^f transition, the B5.2 His residue is displaced by approximately 12 Å and its carbonyl oxygen is now able to accept a proton from the hydroxy group of B16.1 Tyr (O^{η}-O, 2.63 Å). As observed in other $T_3R^f_3$ insulin hexamers (Ciszak & Smith, 1994; Smith & Ciszak, 1994; Ciszak et al., 1995), the first three residues of the N-terminus of the R-state B-chain adopt an extended or R^f conformation. This places the carbonyl oxygen of the B3.2 Asn side chain in a position where it can accept the α-helical hydrogen bonds from the amino nitrogens of both B5.2 His (3.03 Å) and B6.2 Leu (3.12 Å).

[3] The 1 or 2 in the decimal portion of the chain name and residue number refers to the T-state or R^f-state monomer, respectively.

Guest molecule

Unlike all known $T_3R_3^f$ or R_6 hexameric insulins that bind only one guest molecule per R- or R^f-state monomer, *two* molecules of 4-hydroxybenzamide are bound by each R^f-state monomer. The first molecule is located in the primary binding site (binding site I), where its hydroxy group donates a hydrogen to the carbonyl oxygen of A6.2 Cys (2.67 Å) and accepts a proton from the nitrogen of A11.2 Cys (2.92 Å) in a manner nearly identical to that observed for phenol (Derewenda et al., 1989; Smith & Dodson, 1992; Whittingham et al., 1995), *m*-cresol, resorcinol (Ciszak & Smith, 1992), 4′-hydroxyacetanilide (Smith & Ciszak, 1994), and methylparaben (Whittingham et al., 1995). The amide nitrogen of the guest molecule donates a proton to a water molecule (O4), which in turn forms hydrogen bonds to the carbonyl oxygen and a carboxyl oxygen of B13.1 Glu (a T-state monomer) in the adjacent insulin dimer. The dihedral angle between the phenyl ring and the amide group is 19.0°, as compared to 14.6° observed in the small molecule structure of 4-hydroxybenzamide (Kashino et al., 1991). The second 4-hydroxybenzamide molecule, with a dihedral angle of 35.4°, occupies binding site II. The hydroxy group of the second guest molecule donates a proton to the carbonyl oxygen of the first guest molecule while accepting a proton from $N^{\delta 1}$ of B10.2 His. A second water molecule (O33) is within hydrogen bonding distance of both the carbonyl oxygen and the amide nitrogen of the guest molecule in site II, and, at the same time, accepts and donates a proton to the carbonyl oxygen and $N^{\delta 1}$ of B10.1 His, respectively, in an adjacent dimer. Thus, the two guest molecules are involved in an extensive hydrogen bonding pattern between pairs of dimers of the hexamer and two water molecules, illustrated in Figure 2.

The interior surface of the phenolic binding site can be represented as three groups of residues: (1) those that are associated with only site I; (2) those that lie at the interface of the two sites (I/II); and (3) those that are only associated with site II (Table 1). For those hexameric insulin complexes that bind only one phenolic derivative per monomer, sites I and I/II define the phenolic binding site, whereas site II contains only water molecules. The binding site, illustrated in Figure 3, is constructed from residues from four different chains and can be approximated as a cylinder. The top of the cylinder is composed of main-chain atoms in the A6.2–A11.2 loop, as well as the side chain of A16.2 Leu. The central and bottom portions of the cylinder contain residues from segments of the α-helical region of one T-state and two symmetry-related R^f-state B-chains. Two narrow channels provide access to binding site I from the surface of the hexamer. The first has a diameter of approximately 3 Å and is bounded on the top by the A8.2–A10.2 loop and on the bottom by B3.4 and B5.4. The entrance to the second channel is between the

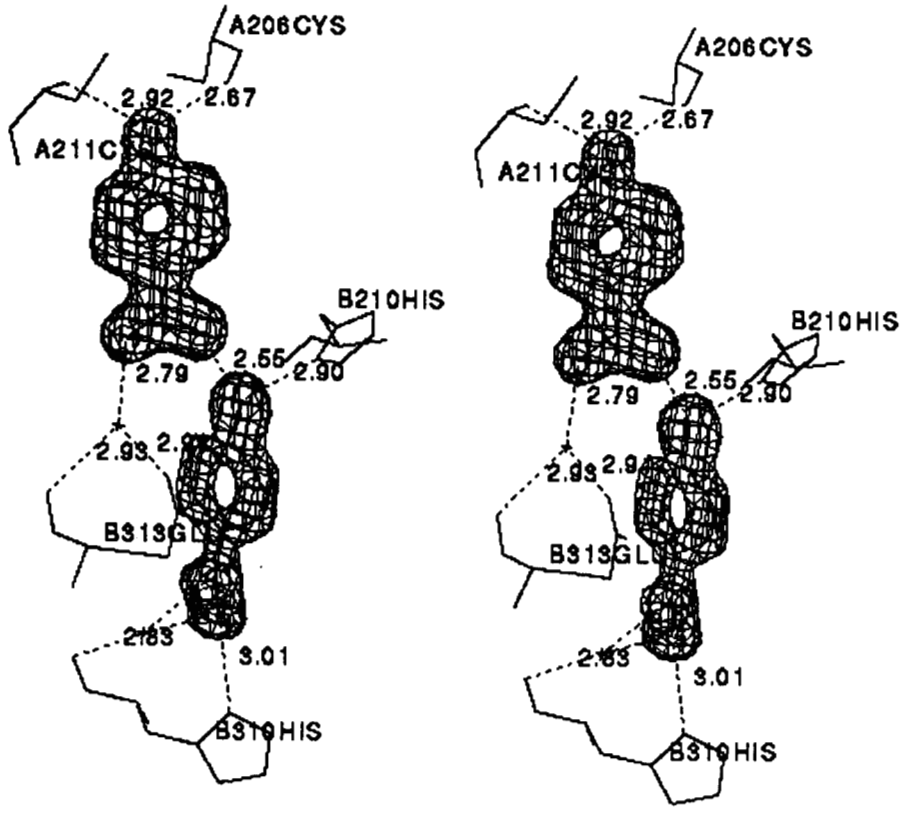

Fig. 2. Stereo pair showing 1.5σ electron density around the pair of 4-hydroxybenzamide molecules in the phenolic binding sites. The 4-hydroxybenzamide molecule in the upper portion of the illustration resides in binding site I, and the second guest molecule resides in binding site II. Water molecules and residues participating in hydrogen bonds are also shown. A206Cys, A211Cys and B210His refer to A6.2 Cys, A11.2 Cys, and B10.2 His, respectively, and B310His and B313Glu refer to B13.1 Glu and B10.1 His of a neighboring dimer.

Table 1. *Identity of the residues that define the interior surface of the phenolic binding sites*[a]

Site I	Site I/II	Site II
A6.2 Cys	B10.2 His	B9.1 Ser
A7.2 Cys	B14.2 Ala	B13.2 Glu
A9.2 Ser	B16.3 Tyr	B16.2 Tyr
A10.2 Ile	B17.3 Leu	B17.2 Leu
A11.2 Cys	B9.4 Ser	B9.3 Ser
A16.2 Leu		B10.3 His
B7.2 Cys		B13.3 Glu
B11.2 Leu		B13.4 Glu
B5.4 His		
B6.4 Leu		

[a] Residue numbers ending with .3 or .4 are related to the T- and R^f-state monomers, respectively, by symmetry.

A10.2–A13.2 and B17.3—B21.3 segments and is approximately 3.5 Å in diameter. Site II can only be accessed from the T_3 side of the hexamer through channels adjacent to the B10 His residues that coordinate to the octahedral zinc ion. The entrance to each of the three channels is bounded on the T_3 trimer surface by B4 Glu, B6 Leu, and B10 His of one monomer and by B5 His and B16 Tyr in two symmetry-related monomers. These three channels join under the zinc ion, as shown in Figure 4, to form a clover-leafed cavity with each lobe separated by a side chain of B13 Glu.

A comparison of the positions of guest molecules in binding site I shows considerable variability. A calculation of the displacements of the carbon atom bound to the hydroxy group in selected guest molecules to that of the position of 4-hydroxybenzamide provides values of 0.51 Å for methylparaben (Whittingham et al., 1995), 0.76 Å for 4′-hydroxyacetanilide (Smith & Ciszak, 1994), 0.70 Å for phenol (Ciszak et al., 1995), and 1.32 and 1.92 Å for the two phenol molecules in the R_6 hexamer (Smith & Dodson, 1992). Although some of these displacements are due to the presence of different functional groups in the guest molecules, some of the larger apparent differences may be due to the lower resolution at which the structures were determined.

Conformational differences—Main chains

Six published TR^f dimers were oriented onto the dimer of the present study by a least-squares procedure minimizing the displacements of the N, C^α, and C atoms of residues B10–B19 of both monomers. Average and RMS displacements of N, C^α, and C for each dimer were calculated and are listed in Table 2, along with an entry for the "2-zinc" T_6 structure. These displacements show that only minor differences exist between the TR^f insulin dimers. The larger displacements for Lys^{B28} Pro^{B29}–human insulin are a result of small conformational perturbations resulting from the sequence inversion at the C-terminus of the B-chain and are discussed in detail in Ciszak et al. (1995). Not surprisingly, the largest displacements are noted at the N- and C-termini of both the A- and B-chains in all six dimers, whereas the smallest displacements are found in the antiparallel β-pleated sheet segment, B24–B26. The conformations of individual A- and B-chains are remarkably similar, in spite of the presence, absence, or the different size of a guest molecule. This is shown in Table 3, in which average displacements are tabulated for residues A3–A20

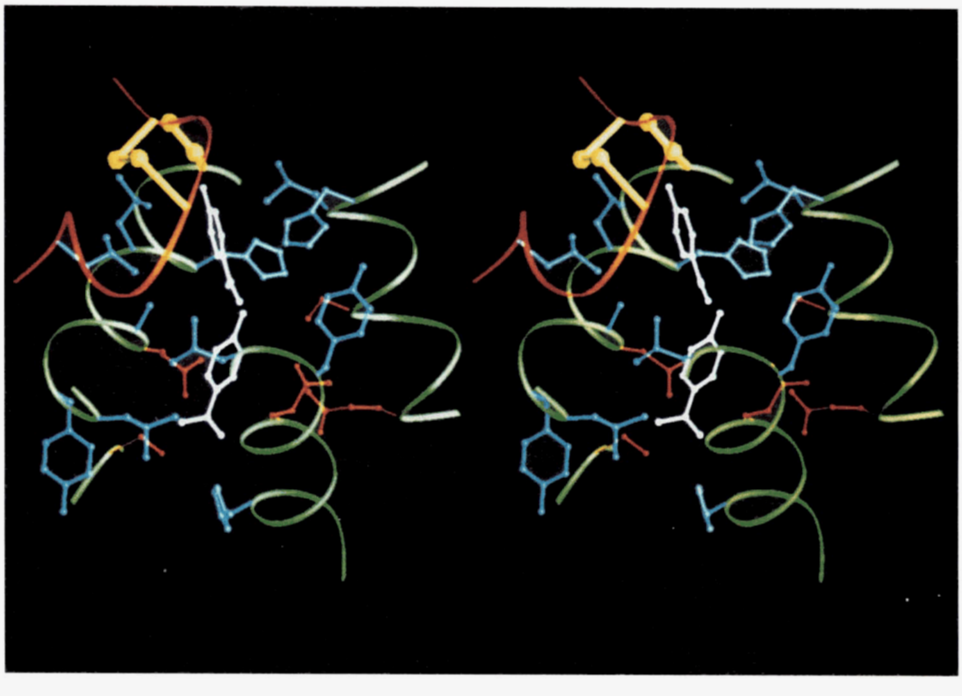

Fig. 3. Stereo plot using Setor (Evans, 1993) of the phenolic binding site along with both 4-hydroxybenzamide molecules. A-chain fragments are colored red; B-chain fragments are green; disulfide bonds are yellow; tyrosine, histidine, leucine, and alanine side chains are blue; glutamate and serine side chains are red; and the pair of 4-hydroxybenzamide molecules are white.

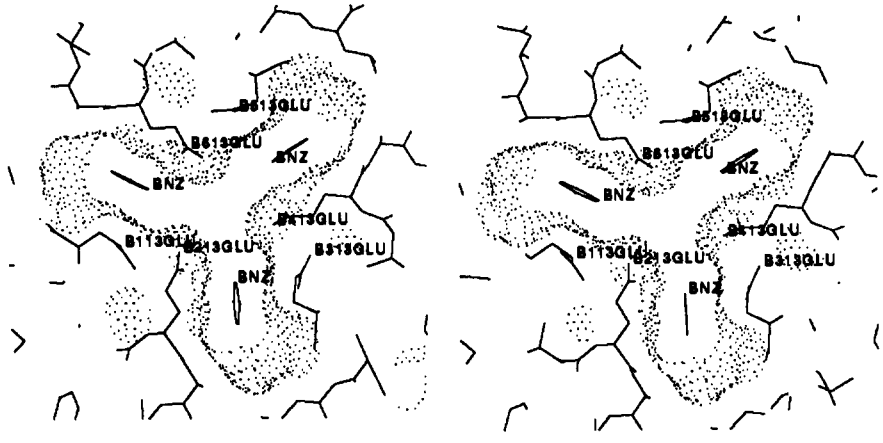

Fig. 4. The bottom portion of binding site II as viewed along the *c*-axis from the T-state trimer toward the R^f-state trimer. The Connolly surface (Connolly, 1983) was constructed from only the protein atoms of the hexamer. The 4-hydroxybenzamide molecule and B13 Glu residues are labeled as BNZ and Bn13GLU, respectively, where n ranges between 1 and 6 and represents B13.n Glu.

or B5–B26 in either the T or R^f conformations; only those residues for which the displacements are listed were minimized in the optimization procedure. The small magnitude of these displacements shows that the binding of two 4-hydroxybenzamide molecules does not distort the conformation of the A- or B-chain backbone atoms in either monomer.

Conformational differences—Side chains

A comparison of the observed side-chain conformations of TR^f dimers, with and without phenolic derivatives, reveals a wide variability for many of the side chains. An examination of side-chain torsion angles shows considerable differences, but in many cases, these different conformations still place a functional group, such as a carboxyl or the terminal methyl groups, in a leucine or valine, in essentially in the same position. However, several side chains, in particular the side chains of B5.2 His and B13.2 Glu, adopt a conformation that is unique to the present study, a result of the presence of the second 4-hydroxybenzamide molecule in site II.

The position of the side chain of B5.2 His in the complexed and uncomplexed $T_3R_3^f$ hexamers is found to fall into two groups. The first group contains the present structure and that of the complex with methylparaben (Whittingham et al., 1995), and a displacement of 0.55 Å exists between the $C^{\epsilon 1}$ atoms of B5.2 His. The second group consists of the two uncomplexed forms (Ciszak & Smith, 1994; Whittingham et al., 1995) and the complexes with phenol (Whittingham et al., 1995) and 4′-hydroxyacetanilide (Smith & Ciszak, 1994), with displacements from $C^{\epsilon 1}$ of B5.2 His of 1.44, 1.26, 1.12, and 1.25 Å, respectively, from that of the present study. Although one might expect the complexes with the larger guest molecules (methylparaben, 4′-hydroxyacetanilide, and 4-hydroxybenzamide) to displace the side chain of B5.2 His from that observed in the uncomplexed forms, 4′-hydroxyacetanilide does not significantly displace this side chain from the positions observed in the uncomplexed forms. However, in the complex with 4′-hydroxyacetanilide, the B5.2 His side chain makes van der Waals contacts with the side chain of A10.2 Ile, and, in fact, forces

Table 2. *Average and RMS displacements (Å) for backbone atoms, N, C_α, and C, of the present study from selected TR^f insulin dimers and the T_2 (2-zinc insulin) dimer*[a]

	B10–B19		All Residues	
Complex	Avg.	RMS	Avg.	RMS
T_2 insulin (4ins)	0.310	0.364	2.221	4.601
TR^f phenol/$K^{B28}P^{B29}$-insulin (1lph)	0.177	0.206	0.508	0.839
TR^f insulin (1trz)	0.129	0.153	0.230	0.404
TR^f thiocyanate/insulin (2tci)	0.120	0.127	0.232	0.318
TR^f phenol/insulin (1mpj)	0.153	0.163	0.295	0.356
TR^f tylenol/insulin (1tyl)	0.148	0.161	0.347	0.530
TR^f tylenol/insulin (1tym)	0.109	0.119	0.205	0.254
TR^f methylparaben/insulin (3mth)	0.124	0.136	0.248	0.320

[a] Displacements of residues B10–B19 of both monomers were minimized in the optimization procedure. PDB entry codes are given in parentheses.

Table 3. *Average displacements (Å) for N, C^α and C for residues A3–A20 (A_T and A_R) and B5–B26 (B_T and B_R) of each monomer from that of the present study*[a]

Complex	A_T	A_R	B_T	B_R
TR^f insulin (1trz)	0.129	0.124	0.121	0.126
TR^f thiocyanate/insulin (2tci)	0.117	0.158	0.090	0.116
TR^f phenol/insulin (1mpj)	0.148	0.165	0.153	0.180
TR^f tylenol/insulin (1tyl)	0.162	0.145	0.088	0.126
TR^f tylenol/insulin (1tym)	0.107	0.117	0.086	0.107
TR^f methylparaben/insulin (3mth)	0.148	0.192	0.149	0.133

[a] Only those residues listed for each chain were minimized in the optimization procedure. The subscript T and R refer to the T-state or R^f-state monomer, respectively. PDB entry codes are given in parentheses.

this latter side chain to adopt a high-energy conformation with $\chi^{1,1} = 133°$. In the present study, the closest contact between B5.2 His and A10.2 Ile is 3.8 Å, and the side chain of A10.2 Ile adopts a low-energy conformation with $\chi^{1,1} = -52.5°$.

The side chains of B13 Glu lie at the central to bottom portion of binding site II. The B13.1 Glu side chains of all $T_3R_3^f$ hexamers appear to form an envelope of conformations that differ only slightly, if the uncomplexed hexamer (Ciszak & Smith, 1994) and the alternate orientations observed in both complexes with 4′-hydroxyacetanilide (Smith & Ciszak, 1994) are ignored. Although the closest contact between the side chain and the guest molecule in site II in the present study is 3.54 Å, distances in the other five hexamers would range from 3.41 Å to 3.11 Å if a guest molecule were present in the site. Thus, this side chain has undergone subtle conformational changes in order to relieve any contacts to the second guest molecule. A wider range of conformations is observed for all of the B13.2 Glu side chains. The closest contact from B13.2 Glu to the second guest molecule is 3.33 Å in the present study, but would range from 1.36 to 2.42 for the remaining six $T_3R_3^f$ hexamers. The larger separation observed in the present study is due primarily to a rotation about the χ^3 torsion angle, which orients the plane of the carboxyl group nearly parallel to the plane of the 4-hydroxybenzamide molecule, as opposed to being more nearly perpendicular in the other structures.

The B22.1 Arg side chain is observed in two discrete conformations. In the primary conformation, $N^{\epsilon 2}$ and $N^{\zeta 2}$ form a salt bridge to an oxygen of the carboxyl group of A21.1 Asn (2.92 and 3.17 Å, respectively); however, the secondary conformation does not participate in salt bridge formation, but rather forms a hydrogen bond to the carbonyl oxygen of B18.1 Val. A salt bridge is also observed between N^{ϵ} of B22.2 Arg and the carboxyl group of A21.2 Asn (2.99 Å).

Disulfide bridges

Torsion angles describing the disulfide bonds for each Cys residue of the present study, for selected $T_3R_3^f$ hexamers, and for the T_6 hexamer are listed in Table 4. The side-chain conformations of A20 Cys and B19 Cys in the T- and R^f-state monomers are virtually identical, as are the disulfide bonds, suggesting that the $T \rightarrow R^f$ transition has no effect upon the conformation of the A20-B19 disulfide bond. However, considerable variation is observed for the other two disulfide links, A6-A11 and A7-B7. As a result of the $T \rightarrow R^f$ transition, χ^1 for both A7.2 Cys and B7.2 Cys undergoes a change of approximately 120°, which alters the handedness of the disulfide bond from right to left, a trend observed for all $T_3R_3^f$ hexamers. The conformation for 15 of the 16 A6 Cys side chains is relatively constant, with χ^1 equal to approximately −54° for both the T and R^f conformations in a TR^f dimer; a single exception is A6.1 Cys in the T_6 hexamer, for which the torsion angle is −71.2°. In the T_6 hexamer, both A11 Cys side chains adopt a conformation with χ^1 equal to approximately 65°. In five of the seven $T_3R_3^f$ hexamers, the χ^1 torsion angle of A11.1 Cys (a T-state monomer) has undergone a rotation of 150° to give a χ^1 torsion angle of approximately −92°; two exceptions are the T-state monomer in the complex with thiocyanate and phenol, for which χ^1 is +90.3 and +80.1°, respectively. The A11.1 Cys residue in the present study is observed in two discrete conformations, with primary and secondary side-chain torsion angles of −84.0° and +69.6°, which is nearly identical to that observed in $T_3R_3^f$ or T_6 state hexamers. The $T \rightarrow R^f$ state transition alters the A11.2 Cys side-chain torsion angle from approximately +65° to −71.6° in the present study, which is agreement with all known $T_3R_3^f$ insulin hexamers.

In the T_6 hexamer, the A6-A11 and A20-B19 disulfide bridges are either completely or partially buried, whereas the

Table 4. *χ^1 ($N\text{-}C^{\alpha}\text{-}C^{\beta}\text{-}S^{\gamma}$) and S-S ($C^{\beta}\text{-}S^{\gamma}\text{-}S^{\gamma}\text{-}C^{\beta}$) torsion angles (°) and the hand of the disulfide bond describing the conformation of the Cys side chains in the T_6 and $T_3R_3^f$ hexamers*[a]

	χ^1_{A6}	χ^1_{A11}	χ^1_{A7}	χ^1_{B7}	χ^1_{A20}	χ^1_{B19}
T-Conformation:						
4ins (monomer 1)	−71.2	64.6	−169.8	−67.8	−56.3	−59.9
(monomer 2)	−56.2	66.1	177.2	−62.9	−54.3	−59.7
1trz	−55.7	−87.4	178.9	−54.9	−60.2	−57.9
2tci	−52.9	90.3	165.3	−55.5	−50.8	−57.2
1mpj	−52.2	80.1	169.3	−59.1	−57.9	−58.3
1tyl	−52.2	−96.4	171.1	−59.5	−49.5	−54.1
1tym	−51.2	−93.5	168.2	−68.2	−53.6	−57.3
3mth	−50.3	−106.0	170.5	−57.6	−63.0	−60.9
Present study	−59.3	−84.0	169.5	−57.1	−54.9	−60.8
		69.6				
R^f-Conformation:						
1trz	−51.8	−64.0	−75.6	−174.7	−53.2	−55.2
2tci	−49.6	−79.5	−67.1	−176.9	−57.1	−53.6
1mpj	−59.9	−65.4	−68.6	177.7	−56.3	−54.6
1tyl	−53.6	−62.4	−69.6	−178.9	−55.3	−48.7
1tym	−55.2	−70.8	−69.6	−173.4	−54.3	−50.9
3mth	−59.5	−77.8	−67.2	−179.9	−55.2	−52.1
Present study	−54.1	−71.6	−65.6	−178.9	−54.9	−60.8

Disulfide torsion angles (°):

	A6-A11	Hand	A7-B7	Hand	A20-B19	Hand
T-Conformation:						
4ins (monomer 1)	109.8	R	101.3	R	−80.6	L
(monomer 2)	107.6	R	101.0	R	−82.6	L
1trz	−75.7	L	94.4	R	−73.8	L
2tci	89.0	R	91.2	R	−72.4	L
1mpj	95.8	R	94.2	R	−74.4	L
1tyl	−62.5	L	98.0	R	−72.0	L
1tym	−69.2	L	93.8	R	−74.9	L
3mth	−54.0	L	93.8	R	−80.3	L
Present study	−81.9	L	97.5	R	−77.4	L
	108.0	R				
R^f-Conformation:						
1trz	−96.7	L	−98.9	L	−82.6	L
2tci	−80.1	L	−95.5	L	−79.2	L
1mpj	−97.6	L	−96.8	L	−77.9	L
1tyl	−96.6	L	−94.0	L	−77.4	L
1tym	−88.5	L	−94.9	L	−81.6	L
3mth	−81.2	L	−95.0	L	−80.5	L
Present study	−86.2	L	−95.1	L	−77.4	L

[a] PDB entry codes refer to the following complexes: 4ins, T_6 uncomplexed insulin (Baker et al., 1988); 1trz, $T_3R_3^f$ uncomplexed insulin (Ciszak & Smith, 1994); 2tci, $T_3R_3^f$ thiocyanate complex (Whittingham et al., 1995); 1mpj, $T_3R_3^f$ phenol complex (Whittingham et al., 1995); 1tyl, $T_3R_3^f$ 4′-hydroxyacetanilide complex (Smith & Ciszak, 1994); 1tym, $T_3R_3^f$ 4′-hydroxyacetanilide complex (Smith & Ciszak, 1994); and 3mth, $T_3R_3^f$ methylparaben complex (Whittingham et al., 1995).

A7-B7 bridge is completely exposed on the surface of the hexamer, where it makes contacts with water molecules. The T-state trimer in the $T_3R_3^f$ hexamer is very similar to that of either trimer of the T_6 hexamer. As a result of the conformational changes that occur during the T → R transition, the placement of the disulfide bonds on or near the surface of the R^f trimer is altered dramatically. Although the accessibility of the A20.2-B19.2 disulfide changes little, the A6.2-A11.2 and A7.2-B7.2 disulfide bridges are only slightly exposed on the surface of the hexamer.

Discussion

The structure of the hexameric insulin complex with 4-hydroxybenzamide provides the first example of a $T_3R_3^f$ insulin hexamer that binds six phenolic derivative molecules. The appearance of the electron density around the guest molecules (Fig. 2) suggests that both sites are fully occupied, and although their mean isotropic temperature factors differ by 20%, they are comparable to the temperature factors of the protein atoms that comprise the binding sites. However, this structure does raise several questions for which the answers are not obvious. The channels that link the two phenolic binding sites to the solvent exterior are too small to accommodate phenol or any phenolic derivative, although, based upon the dimensions of the channel, it would appear that water may be free to migrate to and from the sites. A T-state trimer in a hexamer is inconsistent with the binding of a phenolic derivative because the side chain of B6 Leu occupies the phenolic binding site, and there is no access to the site from the surface of an R-state trimer. This seems to suggest that the conformational flexibility of the first eight residues of the B-chain allows them to move away from the entrance to the binding site, permitting the guest molecule to enter, although this would still require the sequential addition of two molecules in the present case. Movement of these B-chains, in combination with the dissociation of hexamers in solution to smaller aggregates such as dimers and tetramers, which completely exposes the binding site on the dimer surface, would further enhance the binding of guest molecules. It seems unlikely that mixed T and R^f conformations can co-exist within a trimer because very close contacts would result between segments B3–B6 in adjacent monomers and cannot be relieved without major conformational changes in other portions of the monomers. Following the binding of a guest molecule by one monomer, the remaining N-terminal B-chain residues can no longer adopt the T-state conformation, which facilitates their transition to the R^f state, supporting the observed positive cooperativity of the T → R transition within a trimer (Brzović et al., 1994; Bloom et al., 1995; Whittingham et al., 1995).

A comparison of the binding sites in the $T_3R_3^f$ hexamer complexed with 4-hydroxybenzamide to that of the R_6 hexamer complexed with phenol (Smith & Dodson, 1992) clearly reveals that, in addition to the six type I binding sites in the R_6 hexamer, there are only three type II sites. Each type II site links a type I site with its counterpart on the opposite side of the hexamer. In order for an R_6 hexamer to bind a guest molecule in site II, the side chains of A13 Leu, B13 Glu, and B17 Leu must undergo significant conformational changes. There are two ways in which to orient the $T_3R_3^f$ hexamer onto the R_6 hexamer, and, regardless of the orientation, the methyl groups of both B17 Leu residues penetrate into the lower portion of site I and the side chains of both B13 Glu residues are directed into the lower and central portions of site II. Although the side chains of both B13 Glu residues can undergo conformational changes to accommodate a guest molecule without contacting neighboring residues, a change in conformation of B17 Leu would bring it into close contact with A13 Leu. In the $T_3R_3^f$ hexamer with a guest molecule bound in site II, the side chains of B13.1 and B13.2 Glu and B17.1 Leu are rotated away from the two sites, with the side chain of A13.2 Leu undergoing a conformational change to relieve steric interactions with the new position of the side chain of B17.1 Leu. From a structural point of view, there appears to be no reason why 4-hydroxybenzamide does not drive the T → R transition to completion to produce an R_6 hexameric complex. A $T_3R_3^f$ hexamer is produced by the complexation of methylparaben by insulin (Whittingham et al., 1995), but, in this case, the concentration of the guest molecule was approximately 10-fold less than the concentration of phenol required to generate an R_6 hexamer. The concentration of 4-hydroxybenzamide was 0.6 of that of phenol, and the resulting $T_3R_3^f$ hexamer suggests that the gain in energy in binding 4-hydroxybenzamide, unlike phenol, *m*-cresol, or resorcinol, is not sufficient to overcome the negative cooperative effect (Brzović et al., 1994; Bloom et al., 1995).

It was noted (Cutfield et al., 1981) that the T → R transition produces a change in conformation at the A6-A11 and A7-B7 disulfide bonds. In the T-state monomer in the $T_3R_3^f$ hexamer, the χ^1 torsion angles of both A7 and B7 change very little and therefore do not alter the disulfide torsion angle significantly. However, in the R-state monomer, the χ^1 torsion angles of both A7 and B7 are interchanged, that is, A7 Cys adopts the conformation of B7 Cys in the T_6 hexamer, whereas B7 Cys has torsion angles similar to that of A7 Cys. Although the large difference in conformation of one cysteine residue is compensated by the second, the torsion angle of the A7-B7 disulfide bond undergoes a rotation of approximately 180°, altering the handedness from right to left. The side chain of A6 Cys in the T-state conformation in a $T_3R_3^f$ hexamer undergoes a change of nearly 17° from that of monomer 1 in the T_6 hexamer, but the conformation of the side chain of A6 in the R^f-state monomer is nearly identical to that of monomer 2 in the T_6 hexamer. The T → R transition alters the side-chain conformation of A11 Cys in the R^f-state monomer, and hence the handedness of the A6-A11 disulfide bond. A similar situation appears to exist for the T-state monomer in the $T_3R_3^f$ hexamer, with three notable exceptions. The side chain of the T-state A11 Cys in the complex with thiocyanate and phenol (Whittingham et al., 1995) adopts a conformation more nearly like that of the T_6 hexamer, as does the secondary conformation of that residue in the present study. These observations clearly show that a T-state monomer in a $T_3R_3^f$ hexamer is consistent with either of the two observed conformations, left- and right-handed, and should be taken into account in the interpretation of spectral studies that rely upon a signal dependent upon the handedness of a disulfide bond.

Under certain conditions, insulin can irreversibly polymerize to form high molecular weight insoluble aggregates. It has been reported that the presence of certain small molecule reagents such as glycerol or phenol can inhibit this behavior (Grau & Saudek, 1987). The A7-B7 disulfide bond lies on the surface of the T_6 hexamer and also on the surface of the T-state trimer in the $T_3R_3^f$ hexamer. However, the R^f disulfide bridges, A6-A11 and A7-B7, are only slightly exposed on the surface of the hexamer.

If these disulfide bridges are involved in the polymerization mechanism, the loss of their surface accessibility could possibly account for the reduced polymerization in the presence of low concentrations of phenol or other reagents that are capable of inducing the T → R transition. One might expect that the R_6 hexamer would be even less prone to polymerization, but this would require a higher concentration of phenol or the presence of an as yet unidentified compound that is more efficient in inducing the T → R transition.

Materials and methods

Biosynthetic human insulin complexed with zinc was provided by Lilly Research Laboratories. Buffer, salts, and other reagents were purchased and used without further purification. The crystals from which the initial set of data were obtained were grown from a solution at pH 5.7 containing 0.9 mM insulin, 0.05 M sodium citrate, 0.007 M zinc acetate, 0.06 M 4-hydroxybenzamide, and 1.0 M sodium chloride. The crystals belong to space group R3 and were indexed in a hexagonal cell. Intensity data were measured to 1.9-Å resolution using a Rigaku R-AXIS II-C mage plate system and RU-200 rotating anode generator with graphite monochromated CuK_α radiation ($\lambda = 1.54178$ Å) at 290 K. Data were processed through the use of the R-AXIS software.

The unit cell constants are nearly identical to that of uncomplexed $T_3R_3^f$ insulin crystals (Ciszak & Smith, 1994) and the complex with 4′-hydroxyacetanilide, Tylenol (Smith & Ciszak, 1994). An initial model of 752 atoms consisted of the entire A-chain and residues B2–B28 of both monomers of the uncomplexed $T_3R_3^f$ insulin dimer (Ciszak & Smith, 1993); side chains that had been refined in two alternative conformations were excluded. Several cycles of restrained least-squares refinement were performed using PROFFT (Hendrickson & Konnert, 1980; Finzel, 1987), refining an overall B-iso, and resulted in a residual of 0.307. Examination of $2F_o - F_c$ and $F_o - F_c$ maps revealed electron density only within binding site I that could be unambiguously interpreted as a 4-hydroxybenzamide molecule. Additional cycles of refinement, including well-defined water molecules and refining individual isotropic temperature factors, reduced the residual to 0.203.

A second crystal growth experiment was performed in microgravity aboard the shuttle flight STS-60 using the Protein Crystallization Facility (PCF) apparatus. The crystals grown in microgravity were larger, free of inclusions, and very well formed as compared to the previous crystals grown in normal gravity. The microgravity-grown crystals are identical to those grown in the previous crystallizations. Unit cell constants averaged over six crystals are $a = b = 80.72$ Å, and $c = 37.63$ Å. Data to a resolution of 1.4 Å were measured on six microgravity-grown crystals using a Rigaku R-AXIS II-C image plate system and RU-200 rotating anode generator with graphite monochromated CuK_α radiation ($\lambda = 1.54178$ Å) at 290 K. The R-AXIS software was used to integrate the intensities and to apply the Lorentz and polarization factors to the data from each frame. Interframe scale factors for the data from each crystal were calculated using SORTAV (Blessing, 1987), excluding all partial reflections and any reflection for which $|F^2|/\sigma(F^2)$ was greater than 3.0 when F^2 was negative. The full and partial amplitudes and their standard deviations from each frame were multiplied by these scale factors, partials from adjacent frames were summed, and an initial scaling of the six sets of data using SORTAV was done in order to identify gross outliers. At this point, it became apparent that there was an average of more than eight replicate measurements for each independent reflection and, therefore, all partial reflections were omitted from the averaging. Following the exclusion of the gross outliers and the partials, a final pass was then made through all of the data in order to scale and merge all replicate reflections. The final statistics showed that only 74 reflections were measured once, 264 reflections were measured twice, and there was an average of 8.6 replicate measurements for each independent reflection. Details of data measurement and processing are provided in Table 5.

As an initial check for the presence of the guest molecule, $2F_o - F_c$ and $F_o - F_c$ electron density maps were calculated using the partially refined 1.9-Å structure as a model, excluding the 4-hydroxybenzamide molecule. These maps clearly verified the presence of the guest molecule in binding site I, but there was no density corresponding to the second guest molecule. Restrained least-squares refining an overall isotropic thermal parameter, using PROFFT (Hendrickson & Konnert, 1980; Finzel, 1987) and the dictionary of Engh and Huber (1991) as modified by Lamzin, Dauter, and Wilson (1995), was begun using the partially refined 1.9-Å model, but excluding water molecules and those side chains that had been modeled initially as disordered. Throughout the refinement, necessary adjustments were made to the model and water molecules were added with CHAIN (Sack, 1988) in accord with good density and acceptable hydrogen bonds to other atoms. The geometry of the model was monitored continually with PROCHECK (Laskowski et al., 1993). As the refinement progressed, it was noted that electron density, which had been modeled as several water molecules adjacent to the 4-hydroxybenzamide molecule, was strongly suggestive of a second guest molecule. Several additional cycles of refinement were performed, excluding all water molecules in the vicinity of the secondary binding site. The resulting electron density maps clearly revealed density that could be identified un-

Table 5. *Data measurement and processing*

Crystal	Number of image frames	Total data	Independent data	*R*-merge
1	43	26,835	10,782	0.044
2	29	20,146	13,131	0.042
3	35	20,015	14,074	0.042
4	75	34,018	16,960	0.056
5	51	29,480	16,404	0.049
6	45	31,249	16,052	0.056
Final merged data		159,339	18,076	0.066

Resolution range *d* (Å)	Completeness	% Measured data with $F_o \geq 2\sigma(F_o)$
∞–3.0	97	100
3.0–2.5	99	99
2.5–2.0	99	98
2.0–1.8	99	91
1.8–1.6	99	80
1.6–1.5	99	60
1.5–1.4	99	35

ambiguously as a second 4-hydroxybenzamide molecule. The second guest molecule was added and the refinement continued.

Initially, an empirical weighting scheme ($w = 1/\sigma^2$(applied)) was applied to the diffraction data where σ(applied) is linear with respect to $\sin(\theta/\lambda)$, but as the refinement proceeded, it became obvious that a single straight line was not sufficient to model the entire range of ΔF. PROFFT was modified to accommodate two empirical weighting schemes, both as a function of $\sin(\theta/\lambda)$; the first was applied to data between 8 and 1.76 Å, whereas the second was applied to data between 1.76 and 1.4 Å resolution.

Early in the refinement, it was obvious that several side chains existed in more than a single discrete conformation. The side chains of B12.1 Val, B18.1 Val, B22.1 Arg, A9.2 Ser, and B26.2 Tyr were modeled in two conformations and were subsequently included in the refinement. Although the side chain of B21.2 Glu could be modeled in a region of weak electron density, the presence of several regions of density, too close to be water molecules, strongly suggests that there are multiple conformations of this side chain. A persistent ΔF peak in the vicinity of the A6.1-A11.1 disulfide bridge was difficult to model because the inclusion of a second A11.1 Cys side chain resulted in very poor geometry. This was finally remedied by including an entire alternate A11.1 Cys residue, which resulted in good geometry and no positive or negative ΔF density. A similar situation was also observed for A8.2 Thr, and again, the residue was modeled as two threonine residues. No density was observed for residues B29.2 Lys and B30.2 Thr, or for the side chains of A14.1 Tyr, B30.1 Thr, and B2.2 Val. In the final cycles of refinement, $\Delta f'$ and $\Delta f''$ were applied to the zinc and chloride ions; hydrogen atom positions were calculated on the basis of idealized geometry and allowed to refine. The final model consisted of 807 protein atoms, two 4-hydroxybenzamide molecules, two zinc ions, one chloride ion, 125 fully occupied water molecules, and 46 partially occupied water molecules. The refinement converged at a residual of 0.154 for 13,694 independent data with $F \geq 2\sigma(F)$. A $\delta(R)$ plot, constructed with NORMAN (Howell & Smith, 1992), was linear with a slope of 1.52 and an intercept of 0.18; the goodness of fit was calculated to be 1.53 for all data and ranged from 2.11 to 1.39 in 15 equal volume shells of $\sin^3\theta/\lambda^3$. Refinement statistics are given in Table 6. The coordinates have been deposited with the Brookhaven Protein Data Bank (code number 1ben).

Because data were measured from six different crystals, the question arises as to whether the observed disorder in the side chains, as well as in residues A11.1 and A8.2, results from intrinsic disorder in the dimer or from the presence of different conformations in different crystals. Difference and $2F_o - F_c$ maps were calculated using the data from crystal 4 and from crystal 5, the two crystals from which the largest amount of independent data were measured. There was no evidence of significant positive or negative ΔF density in the vicinity of the disulfide bridge (A6.1-A11.1), in the region of A8.2 Thr, or in any of the disordered side chains. One can thus conclude that the observed disorder is intrinsic to the dimer and not a result of merging data from multiple crystals.

Table 6. *Refinement statistics*

Resolution	∞–1.4 Å
No. of reflections ($F > 0$)	18,002
R	0.192
Rw	0.254
No. of reflections ($F_o \geq 2\sigma(F_o)$)	13,789
R	0.171
Rw	0.228
Resolution	8.0–1.4 Å
No. of reflections ($F > 0$)	17,907
R	0.176
Rw	0.215
No. of reflections ($F_o \geq 2\sigma(F_o)$)	13,694
R	0.154
Rw	0.183

	Target Sigmas	Distances (Å)
Bond distances (1–2)	0.020	0.013
Angle distances (1–3)	0.040	0.034
X-H bond distances	0.030	0.009
X-X-H angle distances	0.040	0.013
Planar distances (1–4)	0.050	0.033
Chiral volume (Å^3)	0.150	0.125
Planar groups (Å)	0.025	0.015
Nonbonded distances (Å)		
Single torsion	0.50	0.183
Multiple torsion	0.50	0.224
Possible H-bonds	0.50	0.250
Torsion angles (°)		
Planar	3.5	3.3
Staggered	20.0	14.5
Orthonormal	25.0	14.9
Thermal parameters (Å^2)		
ΔB Main chain	2.00	1.940
ΔB Side chain	2.00	2.021

Acknowledgments

We thank Dr. Marianna Long and Ms. Vickie King for setting up the microgravity crystal growth experiments, Robert H. Blessing for stimulating discussions, and Lilly Research Laboratories for a generous gift of recombinant human insulin. The microgravity crystallization experiments were supported by NASA (NAG-813) and the data measurement, processing, and refinement were supported by NIH grant DK-41387.

References

Baker EN, Blundell TL, Cutfield JF, Cutfield SM, Dodson EJ, Dodson GG, Hodgkin DC, Hubbard RE, Isaacs NW, Reynolds CD, Sakabe K, Sakabe N, Vijayan NM. 1988. The structure of 2Zn pig insulin crystals at 1.5 Å resolution. *Phil Trans R Soc Lond B 319*:369–456.

Blessing RH. 1987. Data reduction and error analysis for accurate single crystal diffraction intensities. *Crystallogr Rev 1*:3–58.

Bloom CR, Choi WE, Brzović PS, Huang JJ, Kaarsholm NC, Dunn MF. 1995. Ligand binding to wild-type and E-B13Q mutant insulins: A three-state allosteric model system showing half-site reactivity. *J Mol Biol 245*:324–330.

Brzović PS, Choi WE, Borchardt D, Kaarsholm NC, Dunn MF. 1994. Structural asymmetry and half-site reactivity in the T to R allosteric transition of the insulin hexamer. *Biochemistry 33*:13057–13069.

Choi WE, Brader ML, Aguilar V, Kaarsholm NC, Dunn MF. 1993. The allosteric transition of the insulin hexamer is modulated by homotropic and heterotropic interactions. *Biochemistry 32*:11638–11645.

Ciszak E, Beals JM, Frank BH, Baker JC, Carter ND, Smith GD. 1995. Role of C-terminal residues in insulin assembly: The structure of hexameric $Lys^{B29}Pro^{B30}$-human insulin. *Structure 3*:615–622.

Ciszak E, Smith GD. 1992. Crystal structures of two new phenolic complexes of insulin. American Crystallographic Association Meeting [Abstr PC46].

Ciszak E, Smith GD. 1994. Crystallographic evidence for dual coordination around zinc in the T_3R_3 human insulin hexamer. *Biochemistry 33*: 1512–1517.

Connolly ML. 1983. Analytical molecular surface calculation. *J Appl Crystallogr 16*:548–558.

Cutfield JF, Cutfield SM, Dodson EJ, Dodson GG, Reynolds CD, Vallely D. 1981. Similarities and differences in the crystal structures of insulin. In: Dodson G, Glusker JP, Sayre D, eds. *Structural studies on molecules of biological interest*. Oxford, UK: Clarendon Press. pp 527–546.

Derewenda U, Derewenda Z, Dodson EJ, Dodson GG, Reynolds C, Smith GD, Sparks C, Swenson D. 1989. Phenol stabilizes more helix in a new symmetrical zinc insulin hexamer. *Nature 338*:589–596.

Engh RA, Huber R. 1991. Accurate bond and angle parameters for X-ray protein structure refinement. *Acta Crystallogr A 47*:392–400.

Evans SV. 1993. SETOR: Hardware-lighted three dimensional solid model representations of macromolecules. *J Mol Graphics 6*:244–245.

Finzel BC. 1987. Incorporation of fast Fourier transforms to speed restrained least-squares refinement of protein structures. *J Appl Crystallogr 20*: 53–55.

Grau U, Saudek CD. 1987. Stable insulin preparation for implanted insulin pumps. *Diabetes 36*:1453–1459.

Hendrickson WA, Konnert JH. 1980. Incorporation of stereochemical information into crystallographic refinement. In: Diamond R, Ramaseshan S, Venkatesan K, eds. *Computing in crystallography*. Indian Academy of Sciences, Bangalore, India. pp 13.01–13.23.

Howell PL, Smith GD. 1992. Identification of heavy-atom derivatives by normal probability methods. *J Appl Crystallogr 25*:81–86.

Kaarsholm NC, Ko HC, Dunn MF. 1989. Comparison of solution structural flexibility and zinc binding domains for insulin, proinsulin, and miniproinsulin. *Biochemistry 28*:4427–4435.

Kashino S, Tateno S, Tanabe H, Haisa M. 1991. Structures of *o*-aminobenzamide and *p*-hydroxybenzamide monohydrate. *Acta Crystallogr C 47*:2236–2239.

Krüger P, Gilge G, Çabuk Y, Wollmer A. 1990. Cooperativity and intermediate states in the T → R-structural transformation of insulin. *Biol Chem Hoppe-Seyler 371*:669–673.

Lamzin VS, Dauter Z, Wilson KS. 1995. Dictionary of protein stereochemistry. *J Appl Crystallogr 28*:338–340.

Laskowski RA, MacArthur MW, Moss DS, Thornton JM. 1993. PROCHECK: A program to check the stereochemical quality of protein structures. *J Appl Crystallogr 26*:283–291.

Sack JS. 1988. CHAIN—A crystallographic modelling program. *J Mol Graphics 6*:244–245.

Smith GD, Ciszak E. 1994. The structure of a complex of hexameric insulin and 4′-hydroxyacetanilide. *Proc Natl Acad Sci USA 91*:8851–8855.

Smith GD, Dodson GG. 1992. The structure of a rhombohedral R_6 insulin/phenol complex. *Proteins Struct Funct Genet 14*:401–408.

Smith GD, Swenson DC, Dodson EJ, Dodson GG, Reynolds CD. 1984. Structural stability in the 4-zinc human insulin hexamer. *Proc Natl Acad Sci USA 81*:7093–7097.

Whittingham JL, Chaudhurri S, Dodson EJ, Moody PCE, Dodson GG. 1995. X-ray crystallographic studies on hexameric insulins in the presence of helix-stabilizing agents, thiocyanate, methylparaben, and phenol. *Biochemistry 34*:15553–15563.